

URBAN DEM

Daniele Perissin, Fabio Rocca

*Politecnico di Milano
Piazza L. da Vinci 32, 20133 Milano, Italy
Email: perissin@elet.polimi.it*

ABSTRACT

The Permanent Scatterers (PS) technique is a powerful operational tool that exploits long series of SAR data for monitoring ground deformations with millimetre accuracy on a high spatial density grid of point-wise targets. The technique has been applied successfully to a number of applications from subsidence and volcano monitoring to slow-landslide detection. Aim of this work is to analyse the location capability of the PS technique, applied to the generation of urban elevation maps. The problem of the univocal identification of the PS position (discarding side lobes) is addressed and an easy and efficient solution is proposed. The results obtained in the Milan site (from ERS and Envisat data coherently combined) allow to appreciate the very high quality of an urban DEM retrieved with the PS technique. The ground level of the city is identified with sub-meter precision, and upper-level targets, where present, reveal the buildings profile. The estimated city street level (ranging $\pm 3m$ in $16 \times 18 km^2$) is then compared with those obtained with the same technique using a descending parallel track and an ascending track.

1 INTRODUCTION

The Permanent Scatterers (PS) technique [1], [2], developed in the late nineties at Politecnico di Milano, takes advantage of long temporal series of SAR data, acquired over the area of interest along the same (nominal) satellite orbit, in order to filter out atmospheric artifacts and to identify a sub-set of image-pixels where high-precision measurements can be carried out.

Even if the theoretical precision of target positioning achievable by means of the PS technique has been already demonstrated being in the order of $1m$ in the three dimensions [1], [2], a proof of it on a large scale has not been produced yet. This is mainly due to difficulties in the association of each coherent pixel to an actual target. In this paper we show that, after discarding redundant pixels, the PS positioning capability can be easily validated.

Exploiting 100 SAR images acquired by the ESA sensors ERS and Envisat over Milan (Italy), PS precise positions estimated through the interferometric phase processing are connected to the sub-pixel positions of the radar return amplitudes of a high number of coherent targets, thus validating the theory. As a consequence, a very precise urban DEM can be obtained. The ground level of the city of Milan is identified with the expected precision of $1m$, and elevated targets, where present, reveal the buildings profile.

The suppression of location ambiguities allows the precise identification of urban radar targets. Thus we discovered that many PS's lie on the ground. This fact can be fruitfully exploited for obtaining an estimate of the city ground level (urban DTM) with a better precision than that achievable for a single target. By averaging the height of nearby PS's the uncertainty can be reduced of a factor proportional to the square root of the number of PS's, thus reaching the tens of centimeters.

Finally, a cross-check of the PS elevation precision has been carried out by comparing three urban DTM's obtained from three different independent tracks over Milan (2 descending and 1 ascending).

2 3D PS POSITIONING

The positioning precision achievable by means of the PS technique has been assessed in the order of $1m$ in the three dimensions in [1], [2], where the PS approach is described in detail. Here we wish to recall briefly only the formulas that apply to the positioning process, in the case of data acquired by 2 sensors with different frequencies (like in the ERS-Envisat case [5], [6]).

Let us consider a pair of co-registered SAR images and the corresponding interferogram. The two images have been acquired with two slightly different carrier frequencies ($f_0, f_0 + \Delta f$), a relative normal baseline B_n and a Doppler centroid (DC) frequency difference Δf_{DC} . With respect to the master image we define as reference system the orthogonal tern formed by the slant range axis r , the azimuth direction y and the cross-slant range axis x normal to the ry plane. The interferometric phase of a point target referred to the center of the sampling cell (neglecting atmospheric artifacts and a possible displacement) is then the sum of three contributions that depend on the target 3D sub-cell position (r, x, y) [5], [6]:

$$\Delta\phi = \frac{4\pi}{c} r\Delta f + \frac{4\pi f_0}{cR_0} xB_n + \frac{2\pi}{PRF\delta_{az}} y\Delta f_{DC} \quad (1)$$

In Eq. 1 c is the light speed, R_0 the sensor-target distance, PRF the pulse repetition frequency and δ_{az} the azimuth sampling step. By means of a multi-interferogram analysis the three terms in Eq. 1 can be separated exploiting their different behavior in the parameter space ($\Delta f, B_n, \Delta f_{DC}$) and the three coordinates (r, x, y) can be estimated. In the case of an ERS-Envisat data-set (31MHz of frequency shift), with 60 ERS and 10 Envisat images, about 500m of normal baseline and 300Hz of DC difference dispersions, it can be shown that the standard deviation of the location estimate is less than 1m in the three dimensions. But without discarding the artifacts coming from the presence of more dependent pixels relative to a single target in a SAR image, such a precision is not actually achievable.

A very simple and efficient solution we found for selecting a single pixel for each real target consists in two steps. First, the local maxima of the incoherent time average of the images amplitude (the so-called reflectivity map) are extracted. Then, dependent side lobes are identified comparing their phase histories. In fact, considering the SAR system impulse response in slant range [3] in a single image n , the phase difference between the main lobe i and the first secondary lobe k is π radians. If the target is a PS, the phase difference between the two lobes is π radians in all N images. We can then evaluate the correlation between the two lobes comparing their phase histories by means of an index like the following one

$$\xi_{i,k} = \frac{1}{N} \left| \sum_{n=1}^N e^{j(\phi_{k,n} - \phi_{i,n})} \right| \quad (2)$$

If the correlation index (Eq. 2) is over a certain threshold, the lobes are considered as dependent and the one with lower amplitude is discarded. It can be shown that, with a data-set like the one previously described, the probability of discarding erroneously a pixel when the correlation index (Eq. 2) is over 0.8 is less than 10^{-5} .

Figure 1a shows the reflectivity map of the area around a very strong scatterer. In Figure 1b 848 pixels have been selected in the area of interest with sufficient amplitude stability. In Figure 1c 88 pixels survive after local maxima extraction. Figure 1d shows that the actual targets are only 41 despite of the initial 848 pixels. In this example the last visible lobe is more than 200m far from the main one and it leads to a height error of 180m.

When artifacts are suppressed, the positioning theory in range and azimuth can be validated comparing the PS sub-pixel location derived from the phase processing (Eq. 1) to the PS sub-cell peak position of the main lobe of the

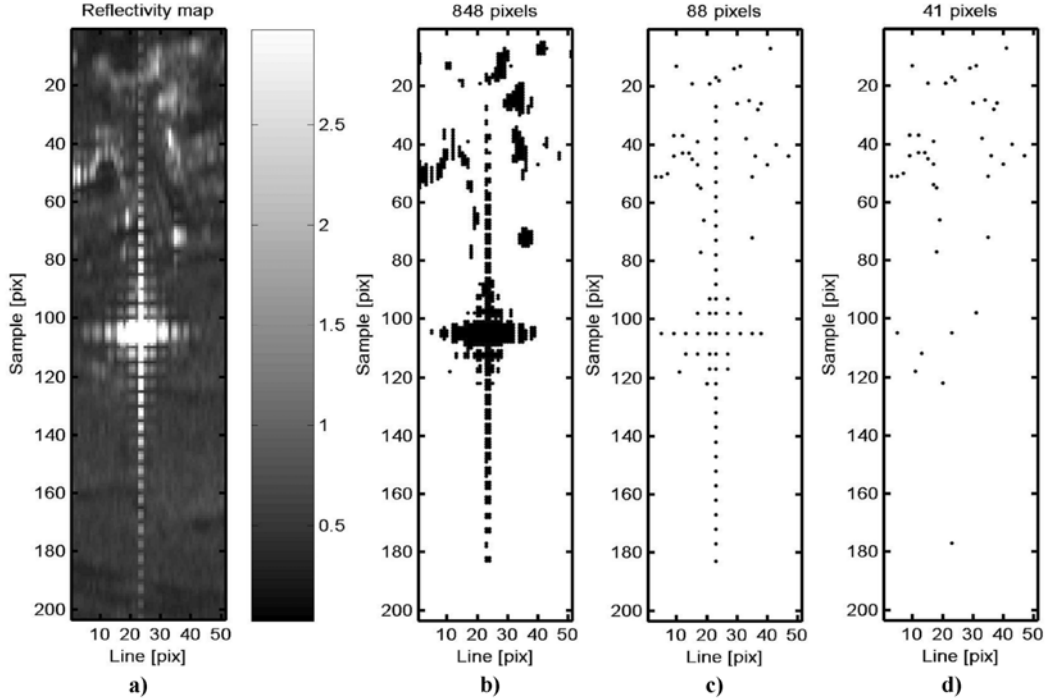


Fig. 1. Example of PSC selection discarding dependent pixels and side lobes. a) reflectivity map of the area around a very strong scatterer; b) 848 pixels have been selected with sufficient amplitude stability; c) 88 pixels survive after local maxima extraction; d) discarding side lobes, the actual targets are only 41.

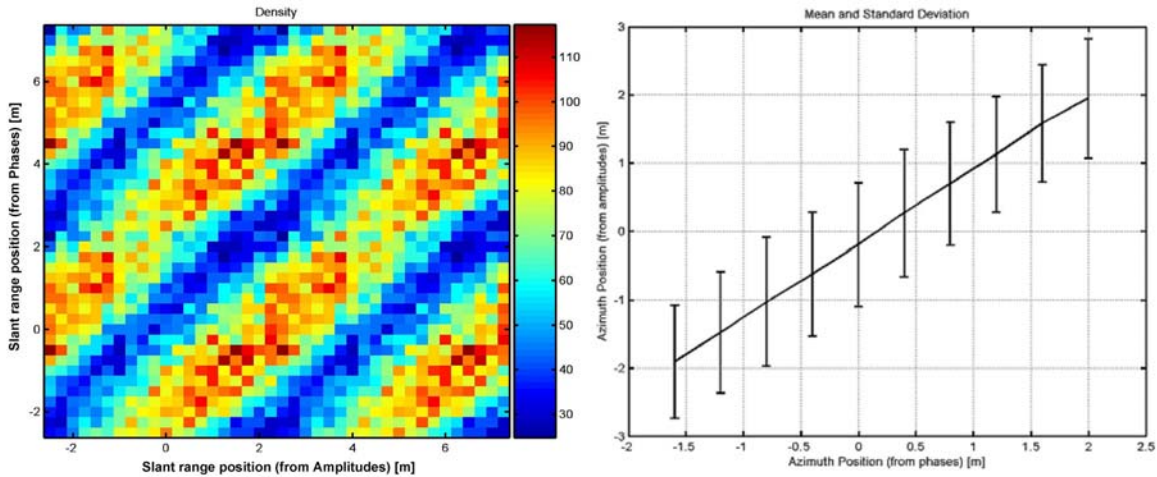


Fig. 2. Left: Cross-plot density between the slant range PS location (y-axis, [m]) derived from the phase processing (ERS-Envisat phase gap) and the position got from the amplitudes peak (x-axis, [m]) of the analyzed PS's. Right: average and standard deviation (sign at $\pm\sigma$) values of the PS azimuth position (got from the amplitudes) as a function of the position obtained from the phase processing, both expressed in meters.

radar response. The chosen test site is the urban area of Milan, which covers about 300 km^2 . About 60,000 PS's have been found with multi-interferogram coherence $\gamma > 0.7$ in 100 images (90 ERS and 10 Envisat, T208 F2691).

Slant range. In Figure 2 on the left we report the cross-plot density between the slant range PS location (y-axis, [m]) derived from the phase processing (first term in Eq. 1, corresponding to the ERS-Envisat phase gap [5], [6]) and the position got from the amplitudes peak (x-axis, [m]) of the analyzed PS's. The ambiguity of the phase measure corresponds to 5m . For visualization purposes, we replicated both quantities at $+5\text{m}$. The good correlation found (dispersion about 1m) is the first proof of the location capability of the PS technique. Moreover, this result demonstrates the physical origin of the ERS-Envisat phase gap [5], [6].

Azimuth. Figure 2 on the right shows average and standard deviation (sign at $\pm\sigma$) values of the PS azimuth position

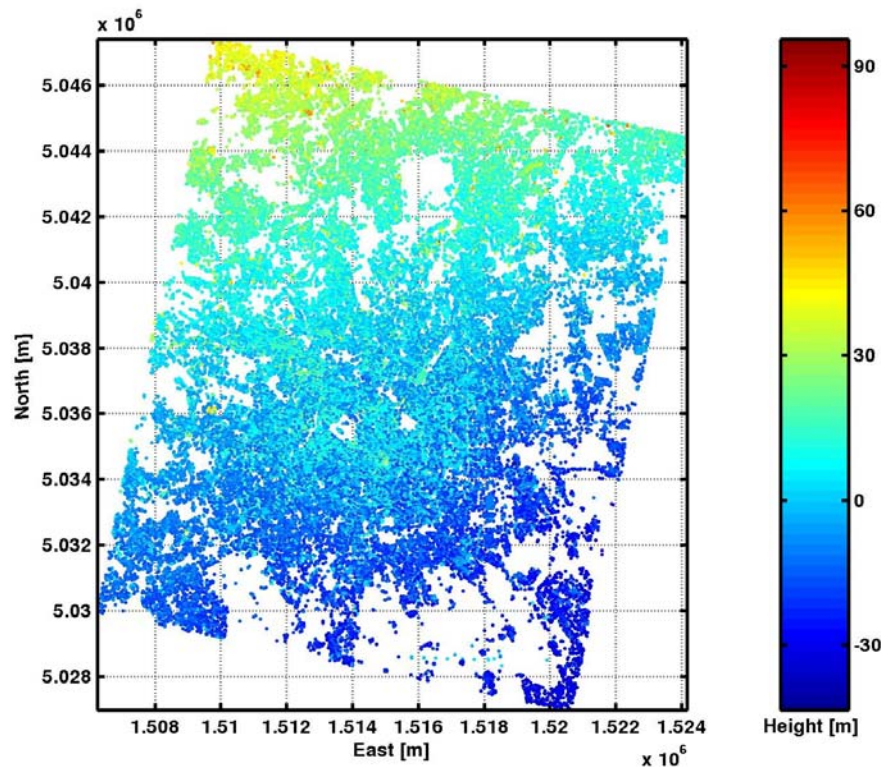


Fig. 3. PS ellipsoidal elevations estimated in Milan (Gauss-Boaga coordinates) with respect to a reference point in the middle of the scene.

(got from the amplitudes) as a function of the position obtained from the phase processing (last term in Eq. 1), both expressed in meters. The estimate dispersion is less than $1m$.

Height. As a consequence, we expect to appreciate very accurate measures of the height of urban targets. In Figure 3 ellipsoidal elevations estimated in Milan are shown (in Gauss-Boaga coordinates). Milano is located on the plain formed by the Po river, which flows to the South of Milan approximately along the West-East direction. Thus, the plain slopes down to South, as visible in Figure 3. In order to evaluate the distribution of the estimated elevations, we divided the analyzed region into smaller areas. In Figure 4 on the left some histograms are reported, calculated on $1km^2$ areas. What's worth appreciating in the left image of Figure 4 is that the height distributions show different modes and that the first mode (lower elevation) has an amplitude always higher than the others. This means that the highest density of PS's is on the ground. The width of the histograms main peak is the first proof of the PS height precision, but it deserves a more accurate analysis.

3 URBAN DTM

The high density of points at "street level" can be exploited for recovering the low-varying topography of Milan (the terrain height). A first rough sampling (1 sample per km^2) of the terrain trend, obtained by extracting the peak positions of the histograms in Figure 4 on the left, is reported in Figure 4 up on the right. A second order surface can then be fitted through the samples, thus obtaining a low-pass synthetic topography (Figure 4 down on the right). By means of the low-pass synthetic topography, PS's around the street level ($\pm 3m$) can be easily selected ($\sim 20,000$ PS's). A sparse set of measures of the ground level is thus available, and it can be used for obtaining an estimate of its trend much more accurate than the estimate of the height of a single target. By averaging N measures with standard deviation σ_s , the resulting precision is $\sigma_r = \sigma_s / \sqrt{N}$. Considering the areas where at least one target is present, the average density of PS's on the ground in the urban site of Milan is about 70 per km^2 . Thus, exploiting e.g. a standard kriging process with a decorrelation distance of $300m$, in a $300 \times 300 m^2$ area the theoretical mean precision of the Milan DTM achievable by means of the PS technique is in the order of tens of centimeters.

Figure 5 up on the left reports the resulting DTM after removal of the low-pass topography. The color scale of the image ranges values between -3 and $3m$. Some interesting feature can be recognized, like a slight prominence (red) in the middle of the image and a couple of depressions aside (blue), extending from north to south.

The DTM just described (Figure 5 up on the left) has been obtained with data acquired from the descending track 208, frame 2691. In Figure 5 two other DTM's of Milan corresponding to the same region but got from different orbits are shown. The first one (up on the right) comes from a different parallel track (T480 F2691), the second one is from an ascending track (T487 F901). The image down on the right is the Milan DTM retrieved from the whole set of PS's detected from the three tracks. All DTM's in Figure 5 have been processed with the previously described technique and the same parameters. Moreover, for a correct comparison, a common low-pass synthetic topography has been removed from all DTM's. As visible in Figure 5, the central slight prominence and the lateral depressions

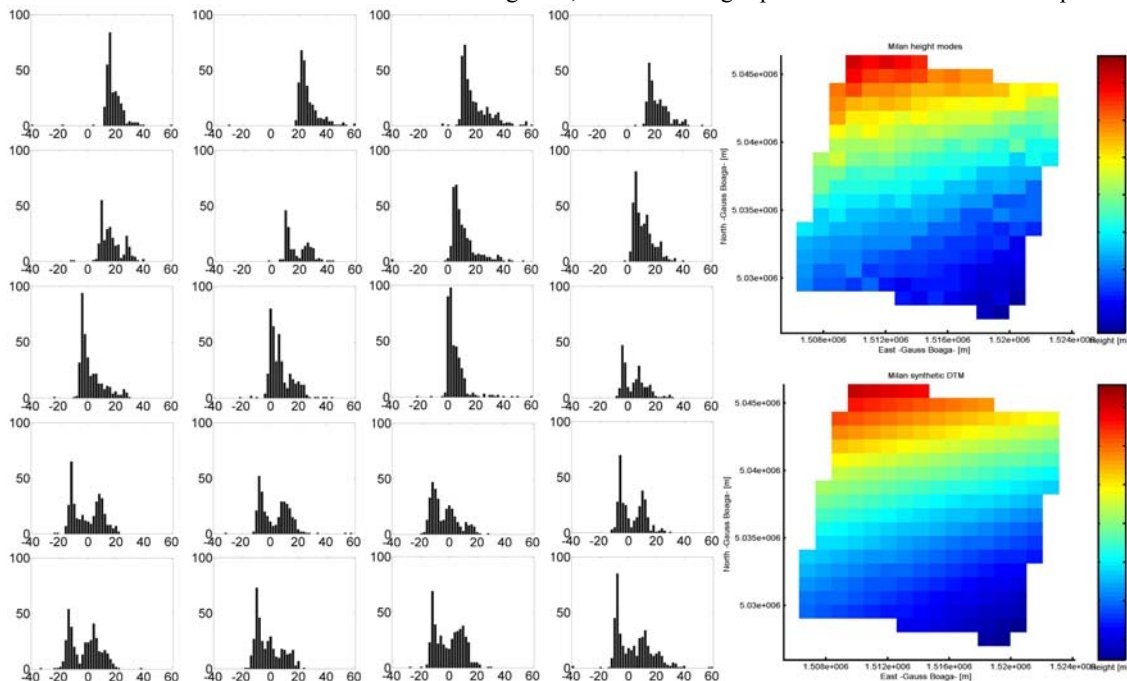


Fig. 4. Left: PS elevation histograms, calculated on $1km^2$ areas. Right up: elevations corresponding to the histogram peaks. Right down: second order surface fitting the data above.

are visible in all images, showing a sub-metrical agreement between the three independent data-set. By combining the data coming from the three different tracks, the average density of PS's on the ground reaches almost 250 per km^2 , thus leading to a theoretical DTM precision of $10cm$ in $200 \times 200m^2$.

The PS precise geolocation of the three tracks has been checked by means of multi-sensor targets like poles, recognized in the Milan site by means of a set of collected radar measurement (see [4] for more details). Figure 6 reports an example of geolocated PS's of the three tracks, showing very impressive details of streets and buildings.

As last proof of the potentiality of the described technique, Figure 7 shows the obtained DTM of Milan together with the georeferenced watercourses in the city. As visible from Figure 7, the detected depressions (blue in the image, $\sim 1m$) previously highlighted are in correspondence of the rivers in Milan. Finally, the red area in the middle of the image identifies the historic center of the city, in the past delimited by walls.

4 CONCLUSIONS

The PS positioning precision has been demonstrated being in the order of $1m$ in the three dimensions and experimental data on a high number of radar targets validate the result. As a consequence, very precise measures of the height of urban scatterers can be provided. Moreover, exploiting the high density of targets on the ground, the city street level can be recovered with tens of centimeters precision. As a proof, three urban DTM's of Milan obtained from three different and independent satellite tracks have been compared showing high correlation. Finally, the detected depressions ($\sim 1m$) in Milan have been found corresponding to the watercourses in the city.

REFERENCES

1. Ferretti, C. Prati and F. Rocca, "Permanent Scatterers in SAR Interferometry", IEEE TGARS, Vol. 39, no. 1, 2001.
2. Ferretti, C. Prati, F. Rocca, "Non-linear subsidence rate estimation using permanent scatterers in Differential SAR Interferometry", IEEE TGARS, Vol. 38, no. 5, 2000.
3. R. Bamler and P. Hartl, "Synthetic aperture radar interferometry", Inverse Problems, vol. 14, pp. R1--54, 1998
4. A. Ferretti, D. Perissin, C. Prati, "Spaceborne SAR anatomy of a city", Proceedings of FRINGE 2005, Frascati (Italy), 28 November - 2 December 2005.
5. M. Arrigoni, C. Colesanti, A. Ferretti, D. Perissin, C. Prati, F. Rocca "Identification of the location phase

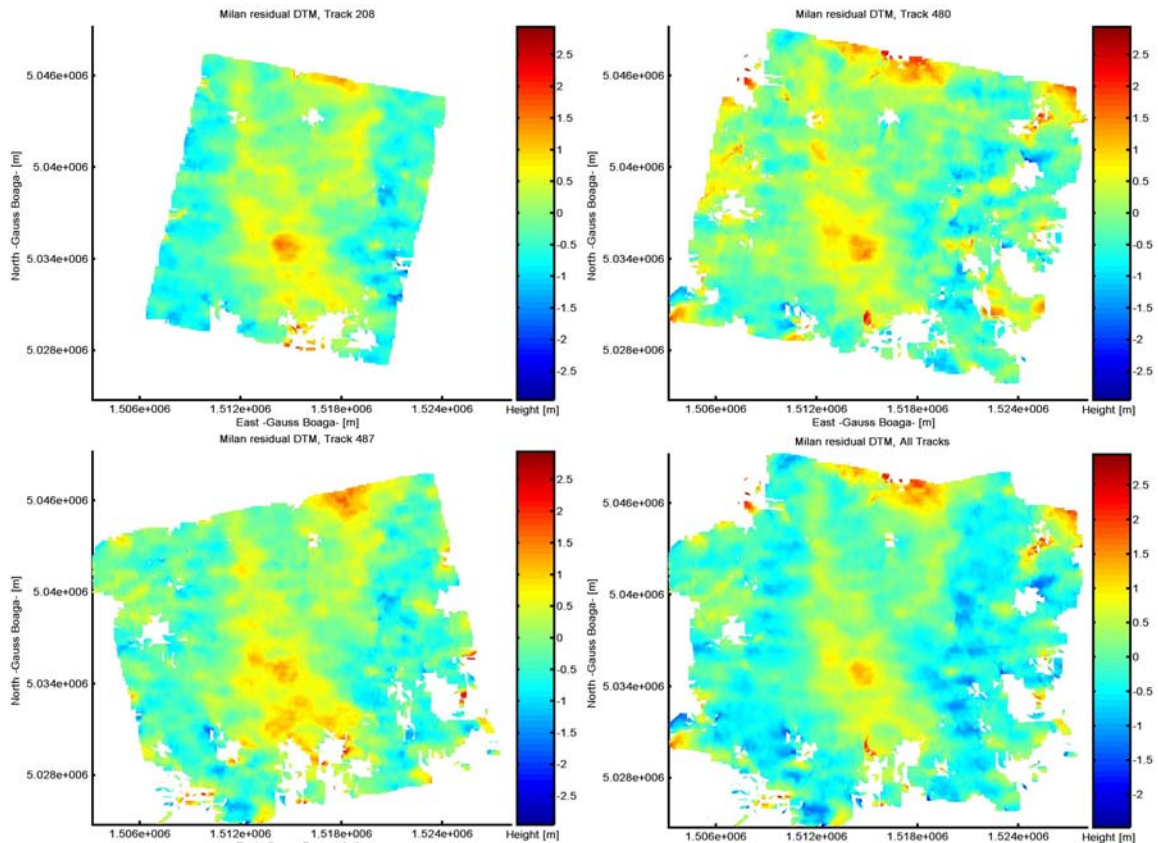


Fig. 5. Residual DTM's of Milan. Up left: Track 208 F2691. Up right Track 480 F2691. Down left: Track 487 F901 (descending). Down right: DTM obtained from the three tracks together.

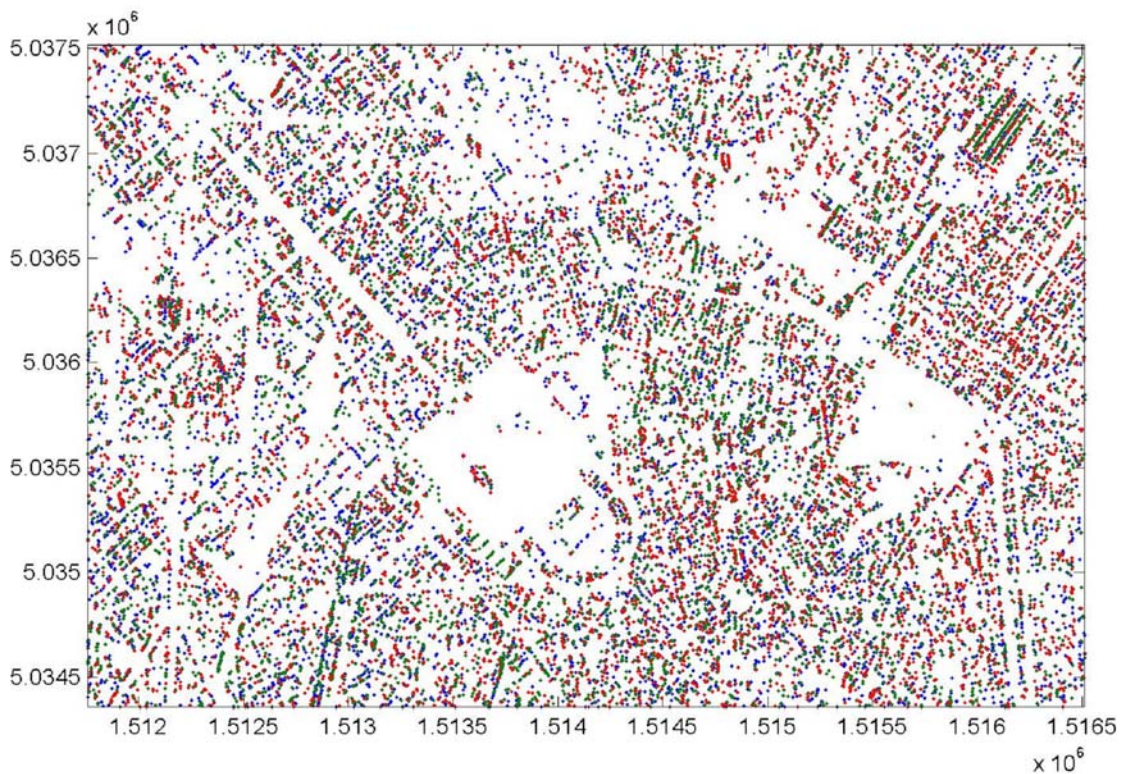


Fig. 6. Georeferenced PS's of the three tracks. Multi-sensor targets [4] are detected by the different tracks with a relative 3D location error lower than 1m.

screen of ERS-ENVISAT Permanent Scatterers”, Proceedings of FRINGE 2003, Frascati (Italy), 1-5 December 2003, ESA SP-550, January 2004.

6. A. Ferretti, D. Perissin, C. Prati, F. Rocca “ERS-ENVISAT Permanent Scatterers”, Proceedings of the IEEE International Geoscience and Remote Sensing Symposium - IGARSS 2004, Anchorage (Alaska), 20-24 September 2004.

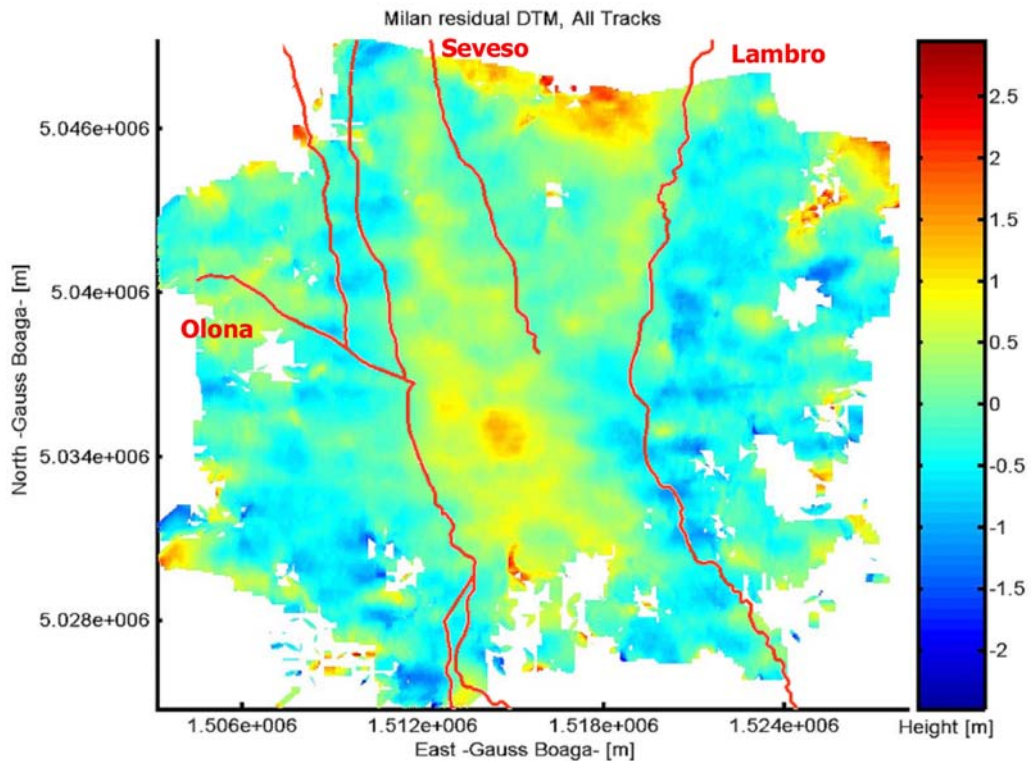


Fig. 7. Milan DTM obtained from the three tracks with the georeferenced watercourses of the city.